Higher-twist term in inclusive pion production at large transverse momentum

E. L. Berger, T. Gottschalk,* and D. Sivers
High Energy Physics Division, Argonne National Laboratory, Argonne, Illinois 60439
(Received 18 August 1980)

We calculate the absolute rate and kinematic dependence of the cross sections for the high-twist subprocesses $qG\to\pi q$ and $q\bar{q}\to\pi G$ in perturbative quantum chromodynamics (QCD). These cross sections are used to estimate the high-twist contribution to large-transverse-momentum inclusive single-pion production in hadronic collisions. We compare the normalization of these terms with leading-order minimum-twist QCD processes such as $qG\to qG$. The high-twist contributions are shown to be quantitatively important for $p_T \lesssim 6$ GeV^2 and $x_T \gtrsim 0.5$, and they should be included in detailed analyses of data. We discuss cross sections and charge ratios, and we comment briefly about inclusive spin-correlation measurements at large p_T.

I. INTRODUCTION

Definite predictions for the production of hadrons at large transverse momentum have been obtained from hard-scattering models based on quantum chromodynamics (QCD).[1-7] The observation that the leading singularities in QCD perturbation theory factor in such a way that they may be absorbed into scale-dependent constituent distribution and fragmentation functions has allowed the calculation of a large number of hard processes.[8] Several groups have investigated in detail the phenomenology of large-p_T hadron production in the framework of leading-order QCD.[9]

The simplest and best known of the hard-scattering predictions is that the 90° cross section should attain the form

$$p_T^4 d\sigma/dp_T^2 = f_a(x_T, \ln(P_T^2/\Lambda^2)). \tag{1.1}$$

Here $x_T = 2p_T/\sqrt{s}$, and f_a is determined from a convolution of calculable cross sections with constituent distribution and decay functions which are, in principle, measurable in other processes. Perturbative QCD predicts two types of corrections to Eq. (1.1). One is logarithmic, $1/\ln(p_T^2/\Lambda^2)$, and the other is of an inverse-power form, m^2/p_T^2. Both types can result in significant modifications of Eq. (1.1). A complication as yet poorly understood is associated with the role of "intrinsic" hadronic constituent transverse momentum and its attendant smearing of $d\sigma/dp_T^2$. Partial calculations of the explicit higher-order perturbative terms which give nonleading logarithmic corrections to large-p_T production indicate that they can be large.[10]

In this paper, we concentrate on the role of high-twist inverse-power terms in inclusive large-p_T single-pion production. As a result of such terms, Eq. (1.1) is replaced by

$$\frac{d\sigma}{dp_T^2} \simeq \frac{f_a(x_T, \ln(p_T^2/\Lambda^2))}{p_T^4} + \frac{f_b(x_T, \ln(p_T^2/\Lambda^2))}{p_T^6} + \frac{f_c(x_T, \ln(p_T^2/\Lambda^2))}{p_T^8} + \cdots, \tag{1.2}$$

where the f's are now convolutions involving non-minimal cross sections and/or generalized multiparton densities.[11,12] Our specific contribution is a detailed evaluation of those p_T^{-6} terms due to the hard-scattering subprocesses $qG \to q\pi$ and $q\bar{q} \to \pi G$, including absolute normalization. In addition to their different dependence on p_T, the high-twist amplitudes provide different expectations for x_T and x_F dependences, as well as different spin and charge correlations from the leading minimum-twist p_T^{-4} term.

It has been emphasized for some time that in a hard-scattering expansion involving *hadrons*, a very significant role may be played by subprocesses involving "constituents" other than the conventional single isolated quarks and gluons.[13,14] Stated otherwise, pairs of quarks or gluons from a given hadron may participate together in a coherent fashion in the hard-scattering process, sharing momentum in a well defined way. Examples include $q + G \to (q\bar{q}) + q$, $q + \bar{q} \to (q\bar{q}) + G$, and $(q\bar{q}) + q \to (q\bar{q}) + q$. Because the processes involve systems such as $(q\bar{q})$, containing more than the minimum number of constituent fields, we label these "higher-twist" processes, in analogy to similar effects identified in the operator-product expansion for deep-inelastic scattering.[15] Recently, Brodsky and Lepage have developed a detailed systematic method for incorporating hadronic binding effects in QCD perturbative calculations.[16]

Although they are suppressed by an inverse power at large p_T, the high-twist cross sections decrease less rapidly as $x_T \to 1$; e.g., as $x_T \to 1$, $f_b/f_a \sim (1 - x_T)^{-2}$ in Eq. (1.2). This is an important compensating advantage. The high-twist subpro-

cesses are enhanced further by "trigger bias."[17] If a hadron is detected with a given p_T, its parent quark or gluon jet must have had even larger p_T. Because the production cross section falls rapidly with p_T, the hadron cross section is suppressed considerably with respect to the jet cross section at the same p_T. By contrast, in the processes $qG \to q\pi$ and $q\bar{q} \to \pi G$, the final π is produced directly, without the necessity of jet fragmentation, and there is no trigger-bias suppression.

Many high-twist processes exist which contribute to the production of a single pion at large p_T. For purposes of classification, we may distinguish high-twist effects associated with the hadronic structure of the initial hadrons[18] from those associated with the final observed pion.[19] All of these effects are potentially significant. The kinematics of large-p_T production probes the initial-hadron structure functions at relatively large values of their fractional momenta x_i, precisely in the kinematic domain in which high-twist and other hadron-wave-function effects are most important. For example, predictions for the x_T and p_T dependences of charge ratios depend on assumptions about the large-x_i dependence of the ratio of up- to down-quark distribution functions $u(x_i)/d(x_i)$. This ratio is affected both by high-twist phenomena and by assumed symmetry properties of the wave functions of the initial hadrons.[20] Expectations for quark- or gluon-*jet* cross sections are also not immune to significant high-twist modifications.

In this modest beginning, we limit the scope of our investigation to those p_T^{-6} high-twist effects associated with the final pion. Furthermore, we examine in detail only the $2 \to 2$ processes ("lowest-order") $qG \to q\pi$ and $q\bar{q} \to \pi G$. These are the only $2 \to 2$ processes giving p_T^{-6} contributions to the cross section. In quark-quark or gluon-gluon scattering, $2 \to 3$ body subprocesses are required: $qq \to \pi qq$, $GG \to \pi q\bar{q}$. Our present results therefore provide a lower bound on the potential size of high-twist effects in high-p_T reactions.

To construct coherent amplitudes for $q\bar{q} \to \pi G$ and $qG \to \pi q$, we follow the methods developed by Farrar and Jackson[21] and extended by Brodsky and Lepage[16] for exclusive hadronic reactions and electromagnetic form factors. The absolute normalization of the rates for $q\bar{q} \to \pi G$ and $qG \to \pi q$ is determined in terms of the pion's weak decay constant f_π or in terms of the pion electromagnetic form factor $F_\pi(Q^2)$ at large Q^2. These procedures, used here for high-p_T amplitudes, have already been tested in other constituent-scattering processes. In particular, the methods were used previously by Berger and Brodsky[18,14] in their treatment of $\pi q \to \gamma^* q$ and lead to a successful prediction of the dominant longitudinal polarization of massive virtual photons[22] in $\pi N \to (l\bar{l})X$ at large x_F. Berger[19] investigated high-twist phenomena in semiinclusive deep-inelastic processes $lN \to l'\pi X$, and predicted joint correlations in the y and z variables which have now been observed.[23] Finally, our approach is consistent with that used by Farrar and Fox[24] in their study of $\pi q \to \pi q$. In contrast to a previous claim,[25] we find that the requirement that the constituent quarks combine to form a color-singlet pion state produces no extraordinary suppression of the cross sections for $q\bar{q} \to \pi G$ and $qG \to \pi q$.

In Sec. II we present an explicit derivation of the amplitudes and cross sections for $q\bar{q} \to \pi G$ and $qG \to \pi q$. We develop two independent ways to normalize the cross sections. The principal method follows the work done on higher-twist phenomena in other reactions, as mentioned above. In the second method, we begin with $2 \to 3$ cross sections [e.g., for $q\bar{q} \to (q\bar{q})G$] and then convolute these with an empirical recombination function for $q\bar{q} \to \pi$. The empirical function is taken from fits to data at low p_T in terms of the quark-recombination model.[26] The normalizations are in good agreement.

In Sec. III we discuss numerical results. We derive some simple analytic approximations which enable us to understand the ratios of different contributions to the overall cross section in the limit $x_T \to 1$. Because we are considering here only a portion of the possible higher-twist effects we do not attempt a complete analysis of data. Nevertheless, we discuss the charge ratio $d\sigma(\pi^- N \to \pi^- N)/d\sigma(\pi^- N \to \pi^+ N)$ since this is sensitive to the presence of higher twist. Using the constituent-interchange model (CIM), Gunion and Jones[27] found a very large value for this ratio, whereas the data show small values consistent with unity.[28] An indication that our normalization of high-twist effects is reasonable is to be found in the fact that our results are consistent with charge ratio data at 90°. There may be a problem in the forward direction, but it is *not* a problem of the normalization of higher-twist effects. Section III also includes a brief discussion of the spin structure of the high-twist subprocess. In $p(\uparrow)p(\uparrow) \to \pi X$ it is possible to define spin-spin asymmetries[29,30] which measure the ability of the constituents to "remember" the proton spin and which are sensitive to the underlying spin dependence of the hard-scattering mechanism. Simple calculations of the helicity amplitudes yield $A_{LL}(q_A\bar{q}_B \to \pi G) = -1$ and $A_{LL}(q_A G \to \pi q_B) < 0$. It may be possible with measurements at large x_T to observe spin effects associated with higher twist.

Section IV includes some discussion of our conclusions.

II. ELEMENTARY PROCESSES

In this section we evaluate the elementary processes

$$q_A\bar{q}_B \to \pi^{\pm} G, \tag{2.1a}$$

$$q_A G \to q_B \pi^{\pm}. \tag{2.1b}$$

We treat only charged-pion production so as to avoid perturbative QCD singularities (which are properly associated with scaling violations). Isospin invariance allows us to extend our results to π^0 production as well.

We will in fact present two different models for these processes, which we label "coherent" and "recombined." In the coherent approach, we calculate a definite underlying $2 \to 2$ scattering amplitude, including an explicit pion wave function. We follow an approach which has been successful in treatments of form factors,[16] large-x Drell-Yan,[18] and other exclusive processes.[16,19] Details of the coherent model are presented in Sec. IIA and will form the basis of all calculations done in Sec. III.

In the recombination approach presented in Sec. IIB, a $2 \to 3$ cross section is convoluted with a probabilistic $q\bar{q} \to \pi$ recombination function, yielding an effective $2 \to 2$ *cross section*. We include this extra calculation primarily to show that our estimates for $q\bar{q} \to \pi G$, $qG \to q\pi$ are not strongly dependent on assumptions concerning the transition from quarks to hadrons. Within the uncertainties inherent in the recombination approach, the results in Sec. IIB are completely consistent with those of Sec. IIA.

In Sec. IIC we summarize the elementary cross sections for (2.1a), (2.1b) in a simple, phenomenologically useful form and make some elementary comparisons.

A. Coherent model

We indicate the coherent-model amplitude by the suggestive notation

$$\langle q_A\bar{q}_B|\pi G\rangle = \langle q_A\bar{q}_B|q_A\bar{q}_B G\rangle \langle q_A\bar{q}_B|\pi\rangle, \tag{2.2}$$

where A, B denote distinct quark flavors. To motivate our specific amplitude for $q\bar{q} \to \pi G$, we consider first the single quark-exchange process sketched in Fig. 1(a). In this $2 \to 2$ process, the pion emerges from an *a priori* complicated $qq\pi$ vertex whose momentum dependence and absolute normalization we wish to specify in some detail.

We take all external particles to be massless and on shell. The transverse momentum of the pion in Fig. 1(a) is thus

$$p_T^2 = \hat{t}\hat{u}/\hat{s}, \tag{2.3}$$

where $\hat{s}$, $\hat{t}$, $\hat{u}$ are the usual $2 \to 2$ invariants. For

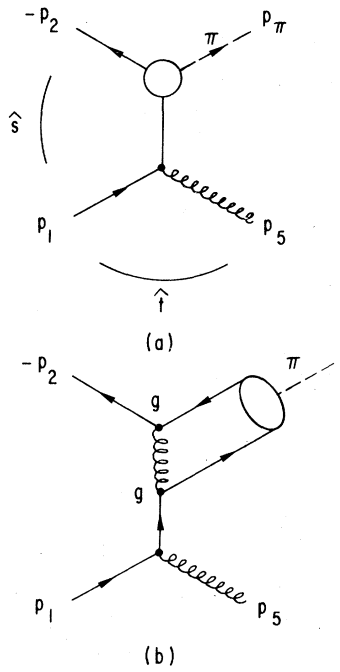

FIG. 1. (a) Single-quark-exchange amplitude for $q\bar{q} \to \pi G$ and (b) hard-gluon approximation for the general $q\bar{q}\pi$ vertex, valid when the exchanged quark is far off shell.

fixed c.m. scattering angle, the exchanged quark in Fig. 1(a) is offshell, carrying squared four-momentum proportional to p_T^2. Thus, if we think of the pion as a $q\bar{q}$ system, the large-p_T process in Fig. 1(a) probes the pion wave function with one of the constituents far off shell. Appealing to the asymptotic freedom of QCD, we represent this large off-shell momentum dependence by the exchange of a single hard gluon, as sketched in Fig. 1(b). The unshaded oval in this figure encompasses all (and only) soft binding effects.[16] Normalization of these soft effects may be obtained in terms of the pion weak decay constant f_π. All hard-scattering effects in Fig. 1(b) are associated with the single exchanged gluon which is off shell by an amount proportional to p_T^2.

The procedure just outlined has been used to obtain a good description of pion-form-factor data.[16] Moreover, it provided a remarkably good prediction for the magnitude and x_F dependence of an unexpected longitudinal polarization of the massive virtual photon in $\pi N \to \gamma^* X$.[14,18]

Additional gluon lines may be inserted in Fig. 1(b). These additional amplitudes are of higher order in the strong coupling and presumably supply logarithmic corrections to our formulas.[16] We will restrict our attention to the exact $O(g^3)$ calculation, including the graph in Fig. 1(b) and its four gauge-invariance partners.

We consider, then, the full underlying QCD amplitude for

$$q_A(p_1,i)+\bar{q}_B(p_2,j)\to q_A(p_3,k)+\bar{q}_B(p_4,l)+G(p_5,a), \tag{2.4}$$

where i, j, k, l, a are color indices. The five contributing graphs are shown in Fig. 2. In Feynman gauge, the amplitude for the first graph, Fig. 2(a), is

$$(p_4-p_2)^2(p_3+p_5)^2\mathfrak{M}_1 = ig^3C_1[\bar{u}(p_3)\gamma^\mu(\not{p}_3+\not{p}_5)\gamma^\alpha u(p_1)] \times[\bar{v}(p_2)\gamma^\alpha v(p_4)]\varepsilon^{\mu *}. \tag{2.5}$$

The color factor is

$$C_1 = (T^b T^a)_{ik}T^b_{ij}. \tag{2.6}$$

The amplitude is simplified when the final $q_A\bar{q}_B$ state is projected onto a state with spin and color quantum numbers of a pion.

Pseudoscalar projection:

$$v(p_4)\bar{u}(p_3)\to\frac{1}{\sqrt{2}}\sum_\lambda v_{-\lambda}(p_4)\bar{u}_\lambda(p_3)=\frac{1}{\sqrt{2}}\not{p}_\pi\gamma_5. \tag{2.7}$$

Color-singlet projection:

$$C_1\to\frac{1}{\sqrt{3}}\sum_{k,l}\delta_{kl}C_1(ijkla)=-\frac{1}{6\sqrt{3}}T^a_{ij}\equiv\tilde{C}_1. \tag{2.8}$$

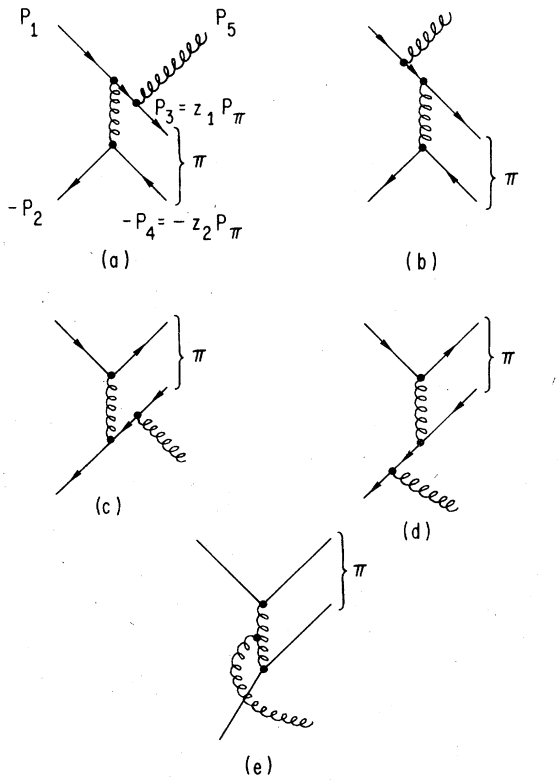

FIG. 2. Full set of Feynman graphs for $q_A\bar{q}_B\to(q_A\bar{q}_B)G$.

For simplicity we ignore "primordial" transverse momentum within the pion. The sharing of longitudinal momentum is expressed through

$$p_3 = z_1p_\pi,\quad p_4 = z_2p_\pi. \tag{2.9}$$

The pion is considered massless: $p_\pi{}^2=0$. Introducing the invariants $\hat{s}=(p_1+p_2)^2$, $\hat{t}=(p_1-p_5)^2$, $\hat{u}=(p_1-p_\pi)^2$, and simplifying the result, we obtain the amplitude

$$\mathfrak{M}_1 = \frac{-ig^3T^a_{ij}}{6\sqrt{6}}\frac{1}{z_1z_2\hat{s}\hat{t}}\varepsilon^{\mu *} \times[-4(p_1-z_2p_\pi)^\mu\bar{v}(p_2)\gamma^5\not{p}_\pi u(p_1) - 2\hat{u}\bar{v}(p_2)\gamma^5\gamma^\mu u(p_1)]. \tag{2.10}$$

Proceeding in a similar manner for the other four graphs in Fig. 2, we obtain for the total $2\to3$ amplitude in Eq. (2.2)

$$\langle q_A\bar{q}_B|(q_A\bar{q}_B)_\pi G\rangle\to\frac{ig^3T^a_{ij}}{6\sqrt{6}}\frac{\tilde{\mathfrak{M}}^\mu\varepsilon^{\mu *}}{z_1z_2\hat{s}\hat{t}\hat{u}}, \tag{2.11}$$

with

$$\tilde{\mathfrak{M}}^\mu(z_1,z_2)=A\bar{v}(p_2)\gamma^5\gamma^\mu u(p_1) + B^\mu\bar{v}(p_2)\gamma^5\not{p}_\pi u(p_1), \tag{2.12}$$

where

$$A = 16z_1\hat{s}\hat{t}-16z_2\hat{s}\hat{u}, \tag{2.13}$$

$$B^\mu = 32\hat{u}p_1^\mu-32\hat{t}p_2^\mu+18(\hat{t}-\hat{u})p_5^\mu + 32(z_1\hat{t}-z_2\hat{u})p_\pi^\mu. \tag{2.14}$$

Note that

$$p_5\cdot B = A\Rightarrow p_5^\mu\tilde{\mathfrak{M}}^\mu=0, \tag{2.15}$$

as is required by gauge invariance. The Eq. (2.12) thus contains all the appropriate "color cancellations" which have been argued previously to suppress the contributions of $q\bar{q}\to\pi G$ and $qG\to q\pi$.[25]

For the pion projection amplitude in Eq. (2.2) we take the asymptotic form[16] [evolved fully in $\ln(Q^2/\Lambda^2)$]

$$\langle q_A\bar{q}_B|\pi\rangle = \sqrt{3}f_\pi z_1z_2\delta(1-z_1-z_2)dz_1dz_2, \tag{2.16}$$

where f_π is the pion weak decay constant, $f_\pi=93$ MeV. A similar procedure yields the correct normalization for the pion form factor.[16,21] Combining Eqs. (2.11) and (2.16) we find

$$\langle q_A\bar{q}_B|\pi G\rangle = \frac{ig^3f_\pi T^a_{ij}}{6\sqrt{2}\hat{s}\hat{t}\hat{u}}\int_0^1 dz_1\varepsilon^\mu\tilde{\mathfrak{M}}^\mu(z_1,1-z_1). \tag{2.17}$$

From this we obtain the spin- and color-averaged squared matrix element

$$F_c(q_A\bar{q}_B \to \pi G) \equiv \tfrac{1}{36} \sum_{\text{colors, spin}} |\langle q_A q_B|\pi G\rangle|^2$$
$$= f_\pi{}^2 g^6 \tfrac{32}{81}(\hat{s}/\hat{u}^2 + \hat{s}/\hat{t}^2)$$
$$= g^6 \frac{f_\pi{}^2}{\hat{s}} \frac{128}{81}\left[\frac{1}{(1+\cos\theta)^2} + \frac{1}{(1-\cos\theta)^2}\right], \tag{2.18}$$

where $\cos\theta \equiv \cos\theta_{\text{c.m.}}(q_A, \pi)$. The expected "higher-twist" scale dependence is present in the form $f_\pi{}^2/\hat{s}$. Note that the normalization in Eq. (2.18) involves no free parameters.

Finally, we may obtain the corresponding mean-squared matrix element for $q_A G \to q_B \pi$ either *ab initio* or by a simple crossing, $\hat{s} \leftrightarrow -\hat{t}$:

$$F_c(q_A G \to q_B \pi) = f_\pi{}^2 g^6 \tfrac{4}{27}[-\hat{t}/\hat{s}^2 - \hat{t}/\hat{u}^2] \tag{2.19}$$
$$= g^6 \frac{f_\pi{}^2}{\hat{s}} \frac{2}{27}(1-z)\left[1 + \frac{4}{(1+\cos\theta)^2}\right],$$

where $\cos\theta \equiv \cos\theta_{\text{c.m.}}(q_A, q_B)$.

It is useful to recall at this point the results of a QCD analysis of the pion electromagnetic form factor.[16] At large Q^2, one obtains

$$F_\pi(Q^2) = 16\pi\alpha_s(Q^2) f_\pi{}^2/Q^2. \tag{2.20}$$

Thus, both Eqs. (2.18) and (2.19) can be reexpressed in terms of $F_\pi(\hat{s})$, eliminating $f_\pi{}^2$.

As in the case of the form factor, Eqs. (2.18) and (2.19) are modified by modest logarithmic effects ($\ln \hat{s}/\Lambda^2$) when the full Q^2 evolution of the pion wave function Eq. (2.16) is incorporated.[16] We will ignore such logarithmic corrections throughout this paper.

B. Recombination model

The results in Eqs. (2.18) and (2.19) depend not only on perturbative QCD *per se*, but also on the assumption that the $q\bar{q}$ representation in Fig. 1(b) provides a quantitative description of physical pions. While the methods used above have enjoyed success, it is nonetheless worthwhile to investigate the extent to which our results are sensitive to the manner in which we append hadrons to a theory which does not yet contain them. With this in mind, we now digress briefly from the main line of this paper and recompute the mean-squared matrix elements for (2.1a) and (2.1b) using a rather different, "softer" picture of the transition from quarks to pions. The principal conclusion of this exercise is that our results are *not* strongly dependent on details of the hadronization model for $q\bar{q} \to \pi$. The discussion below is self-contained and, without serious loss of content, the reader may prefer to skip directly to Sec. II C.

Turning to specifics of the recombination approach, we begin with the perturbative QCD cross section for the $2 \to 3$ process $q_A\bar{q}_B \to q_A\bar{q}_B G$. For distinct flavors $A \neq B$ it is easy to see that the lowest-order $2 \to 3$ cross section is finite and well behaved for $m_{AB}{}^2 = (p_A + p_B)^2 \to 0$. Given the existence of $2 \to 3$ processes in the theory, it is possible to compute the cross section for production of an approximately collinear, on-mass-shell quark-antiquark pair. As pictured in Fig. 3, the quark and antiquark can then produce hadrons either by fragmenting individually or by recombining to form a single meson with the combined momentum of the pair. This recombination is not a short-distance effect and thus is not calculable in perturbation theory. However, if we assume that recombination is a universal phenomenon, we can use the quark-recombination probabilities obtained by Das and Hwa,[26] by DeGrand and Miettinen,[31] and by others[32] in the study of pion production at low p_T. In contrast to the coherent model of the previous section, the recombination model leads to a probabilistic, incoherent approximation

$$|\langle q_A\bar{q}_B|\pi G\rangle|^2 = |\langle q_A\bar{q}_B|q_A\bar{q}_B G\rangle|^2 |\langle q_A\bar{q}_B|\pi\rangle|^2. \tag{2.21}$$

We now address spin and color constraints in the recombination model. There are two approaches to this question, and we will consider both in order to put to rest any confusion about the role of color projection. In the usual recombination model[26] the spins and colors of the quark and antiquark in Fig. 3 are assumed to be uncorrelated. The requirement that the produced pion be a color-singlet pseudoscalar is incorporated in the nor-

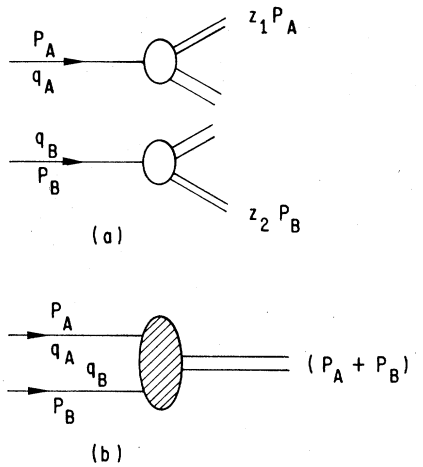

FIG. 3. Mechanisms for hadron production from a parallel quark-antiquark pair: (a) individual hadronization and (b) quark recombination.

malization of the recombination function

$$|\langle q_A\bar{q}_B|\pi\rangle|^2 \equiv R_\pi(z_1,z_2) = a_\pi z_1 z_2 \delta(1-z_1-z_2), \quad (2.22)$$

with $a_\pi \simeq 1$.[26,31,32] Thus, if we use the $2\to 3$ color- and spin-summed QCD cross section and convolute with Eq. (2.22), we obtain a consistent normalization of the effective $q_A\bar{q}_B \to \pi G$ cross section.

Alternately, we can recompute the $2\to 3$ cross section in Eq. (2.21) projecting out the color-singlet component of the final-state $q\bar{q}$ pair and inserting a factor $\frac{1}{4}$ to account (statistically) for the projection of spins. The two-jet system in Fig. 3 thus has the quantum numbers of a pion. If the two jets are sufficiently close in invariant mass, the probability that they will recombine to form a pion should approach unity. The normalization of the singlet-projected recombination function is thus determined:

$$\int dz_1 dz_2 \tilde{R}(z_1,z_2) \simeq 1 = \int_0^1 dz_1\, \tilde{a}_\pi z_1(1-z_1). \quad (2.23)$$

This procedure yields $\tilde{a}_\pi \simeq 6$. This explicit color-singlet modification of the recombination model is reminiscent of the "preconfinement" picture[33] of hadronization inspired by leading-logarithm perturbative QCD. In essence, we have simply identified a sufficiently small mass color singlet with an individual hadron.

To implement the recombination model, we first need the spin- and color-averaged squared amplitudes for the underlying $2\to 3$ processes. The required spin sums are evaluated in Ref. 34. The modifications imposed by the color-singlet restriction are discussed in the Appendix. For the present, we restrict consideration to the color-averaged process $q_A\bar{q}_B \to q_A\bar{q}_B G$, and define

$$H \equiv \tfrac{1}{36} \sum_{\text{color, spins}} |\mathfrak{M}(q_A\bar{q}_B \to q_A\bar{q}_B G)|^2, \quad (2.24)$$

where $\mathfrak{M}$ is the full $2\to 3$ QCD amplitude. We again simplify the kinematics and use the parallel-configuration replacements in Eq. (2.9). It is straightforward to obtain

$$H = \frac{64}{27}\,\frac{q^6 \tilde{H}}{z_1 z_2 \hat{s}\hat{t}^2\hat{u}^2}, \quad (2.25)$$

with

$$\tilde{H} = z_1 z_2 \hat{s}^2(4\hat{u}^2+4\hat{t}^2+\hat{u}\hat{t}) - 3z_1\hat{s}^2(\hat{u}^2-\hat{t}^2) + \hat{t}^2\hat{u}^2 + 6\hat{s}^2\hat{t}^2 - 8\hat{s}^3\hat{u} + \hat{s}^3\hat{t}, \quad (2.26)$$

where the invariants $\hat{s}$, $\hat{t}$, $\hat{u}$ are as defined after Eq. (2.9).

In order to combine Eqs. (2.22) and (2.26), we first simplify the $2\to 3$ phase space for $q_A\bar{q}_B \to q_A\bar{q}_B G$:

$$d_3P(1+2\to 3+4+5) \equiv (2\pi)^{-5}\prod_{j=3}^{5}\frac{d^3p_j}{2E_j}\,\delta^{(4)}(p_1+p_2-p_3-p_4-p_5) = d_2P(1+2\to X+5)\,\frac{dm_X^2}{2\pi}\,d_2P(X\to 3+4), \quad (2.27)$$

where X is identified with the final $q_A\bar{q}_B$ pair. In the parallel-kinematics approximation we may replace

$$dm_X^2/2\pi \to \Delta m^2/2\pi, \quad (2.28)$$

$$d_2P(X\to 3+4) \to \frac{1}{8\pi}\,dz_1. \quad (2.29)$$

The parameter Δm^2 in Eq. (2.28) is a maximum-mass cutoff for identifying the final-state $q\bar{q}$ system with a single hadron.

Using Eqs. (2.28) and (2.29) we obtain the effective $2\to 2$ mean-squared matrix element

$$F_I(q_A\bar{q}_B \to \pi G) \equiv |\langle q_A\bar{q}_B|\pi G\rangle|^2 \quad \text{(color averaged)}, \quad (2.30)$$

$$F_I = \frac{\Delta m^2}{2\pi}\,\frac{1}{8\pi}\int dz_1 dz_2 H(z_j)R(z_j) = \frac{g^6}{16\pi^2}\,\frac{8}{729}\,\frac{a_\pi \Delta m^2}{\hat{s}}\,\frac{(2\hat{t}^2+2\hat{s}\hat{t}+5\hat{s}^2)(3\hat{t}^2+3\hat{s}\hat{t}+7\hat{s}^2)}{\hat{s}\hat{t}^2\hat{u}^2}$$

$$= g^6\,\frac{a_\pi \Delta m^2}{16\pi^2\hat{s}}\,\frac{16}{729}\,\frac{(\cos\theta^2+9)(3\cos\theta^2+25)}{(1-\cos\theta)^2(1+\cos\theta)^2} \quad (2.31)$$

with $\cos\theta$ as defined after Eq. (2.18). Results for the other color-averaged process and for both color-singlet processes are quite similar and are listed in the next section.

Note that, unlike the coherent model, the normalization of Eq. (2.31) is somewhat uncertain due to the cutoff Δm^2. We will use $\Delta m^2 = (0.5\ \text{GeV})^2$ as a plausible value in subsequent calculations.

C. Elementary cross sections

We now summarize and compare the elementary pion-production cross sections resulting from the mechanisms described in the preceding sections. These can be written in the general form

$$\frac{d\sigma}{d\hat{t}}(ab\to c\pi) = \frac{\pi\alpha_s^2}{\hat{s}^2}\,\frac{\alpha_s}{4\pi}\,\frac{s_0}{\hat{s}}\,F(\cos\theta), \quad (2.32)$$

where s_0 is a higher-twist scale fixed by the models, and the c.m. scattering angle is defined by

$$\hat{t} = -(1-\cos\theta)\hat{s}/2 . \tag{2.33}$$

For comparison, recall that an elementary $2\to2$ QCD cross section (e.g., for $qq\to qq$) is of the form

$$\frac{d\sigma}{d\hat{t}}(ab\to cd) = \frac{\pi\alpha_s^2}{\hat{s}^2} B(\cos\theta), \tag{2.34}$$

where $B \equiv \langle |M|^2\rangle/g^4$.

Coherent model. The higher-twist scale s_0 is

$$s_0 = 16\pi^2 f_\pi^2 . \tag{2.35}$$

The angular functions F in Eq. (2.32) are

$$q_A\bar{q}_B\to\pi G:\quad F(z) = \frac{256}{81}\frac{1+z^2}{(1-z)^2(1+z)^2}, \tag{2.36}$$

$$\hat{t} \equiv (p_{q_A} - p_G)^2; \tag{2.37}$$

$$q_A G\to q_B\pi:\quad F(z) = \frac{2}{27}(1-z)\left[1+\frac{4}{(1+z)^2}\right], \tag{2.38}$$

$$\hat{t} \equiv (p_G - p_\pi)^2 . \tag{2.39}$$

Recombination models. Here the scale s_0 is

$$s_0 = a_\pi \Delta m^2 . \tag{2.40}$$

Keeping the angle assignments used above, we have

$$q_A\bar{q}_B\to\pi G:\quad F(z) = \frac{16}{81}\frac{(z^2+7)(z^2+15)}{(1-z)^2(1+z)^2}\quad\text{(color averaged)}, \tag{2.41}$$

$$F(z) = \frac{16}{729}\frac{(z^2+9)(3z^2+25)}{(1-z)^2(1+z)^2}\quad\text{(color singlet)}; \tag{2.42}$$

$$q_A G\to q_B\pi:\quad F(z) = \frac{4}{27}\frac{(z^2-z+2)(2z^2-3z+3)}{(1-z)(1+z)^2}\quad\text{(color averaged)}, \tag{2.43}$$

$$F(z) = \frac{1}{486}\frac{(5z^2-6z+9)(7z^2-8z+13)}{(1-z)(1+z)^2}\quad\text{(color singlet)}. \tag{2.44}$$

In Fig. 4 we show results for $(\alpha_s/4)\, s_0 F$ for all models and processes with $\alpha_s = 0.25$, $\Delta m^2 = (0.5\ \text{GeV})^2$, and $f_\pi = 93$ MeV. As discussed in the preceding section, the constants in the recombination model are $a_\pi = 1$ (color averaged) and $a_\pi = 6$ (color singlet). Several comments are now in order.

(1) In the region relevant for high-p_T physics, say $|\cos\theta_{\text{c.m.}}| < 0.6$, we find that

$$F(q\bar{q}\to\pi G) \gg F(qG\to q\pi) . \tag{2.45}$$

Thus, the particular higher-twist mechanisms we are studying will be more important in $\pi N\to\pi X$, $\pi p\to\pi X$, and $\bar{p}p\to\pi X$ than in $pp\to\pi X$.

(2) The angular functions have strong forward and/or backward poles (comparable to those of $2\to2$ QCD squared matrix elements). The double poles correspond to zero-angle scattering of one of the pion constituents. In contrast, for $\cos\theta = 1$ in $q_A G\to q_B\pi$, q_A has been scattered through 180°, and the cross sections are greatly reduced. The coherent-model amplitude for $qG\to q\pi$ vanishes for $\cos\theta = 1$, as expected from a simple helicity argument.

(3) Except for the very forward region for $qG\to q\pi$, the coherent- and recombination-model predictions are extremely similar in both angular dependence and magnitude. It is interesting in this regard to note the similarity of the effective higher-twist scales s_0 in Eq. (2.35) and (2.40), with $s_0 \simeq (1\ \text{GeV})^2$.

(4) When differences due to the values of a_π and the statistical spin factors are removed, the color-singlet restriction does *not* significantly decrease the cross section. Because this is contrary to expectations based on a simple examination of the color factors,[25] the result is discussed in more detail in the Appendix.

Finally, to give some meaning to the vertical scale in Fig. 4, we note the typical $2\to2$ constants B in Eq. (2.34) at 90°:

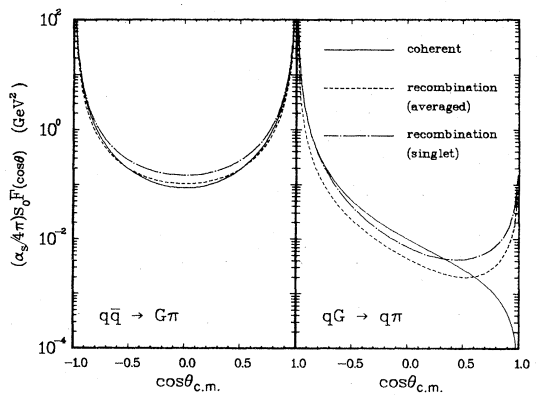

FIG. 4. Angular dependence of the higher-twist squared matrix elements for $q\bar{q}\to\pi G$, $qG\to q\pi$.

$$B(O)=\begin{cases}\frac{20}{9} & (q_A\bar{q}_B\to q_A\bar{q}_B),\\ \frac{55}{9} & (q_AG\to q_AG).\end{cases} \tag{2.46}$$

Incorporating the higher-twist denominator $\hat{s}^{-1}$ in Eq. (2.32), we thus estimate a typical suppression of $10^{-2}-10^{-3}$ for higher twist vs $2\to 2$ minimal-twist QCD at currently accessible energy scales. However, if we incorporate the known particle-jet suppression for $2\to 2$ QCD plus fragmentation (typically 10^2), we expect that the higher-twist single-particle yield is *not* negligible, particularly at large x_T. In the next section, we provide specific quantitative expectations.

III. NUMERICAL ESTIMATES

A. Objectives

Our aim in this section is to provide quantitative estimates for the magnitude of higher-twist modifications to cross sections and charge ratios at large p_T. It would be most illuminating to confront the high-twist cross sections directly with data. However, to make such a comparison meaningful, we would have to deal in detail with at least two significant problems. These are (i) smearing of the predicted p_T dependence associated with the intrinsic k_T of initial constituents, and (ii) modifications (damping) of our expected p_T^{-6} dependence associated with logarithmic $\ln(p_T^2/\Lambda^2)$ scale breaking in the initial-hadron structure functions. Furthermore, direct comparison with data at this point is premature. As discussed in the Introduction, we are aware that we have evaluated too few of the potentially significant high-twist terms. Instead, we shall compare our high-twist cross sections with yields expected from mimimum-twist $2\to 2$ QCD processes. In other words, we intend to compare the behavior of the p_T^{-4} and p_T^{-6} terms in Eq. (1.2), in an attempt to ascertain over what range of the kinematic variables the high-twist term is expected to be a significant "correction."

Our procedure is not without ambiguity. For example, we are still required to make choices of structure functions. However, these choices affect both the $2\to 2$ minimum-twist and higher-twist cross sections in roughly the same way, and one may hope that subtleties cancel in the comparison. We will ignore intrinsic k_T smearing altogether. The principal source of uncertainty in the comparison is associated with our choice of quark-to-pion or gluon-to-pion fragmentation functions. We need such functions in order to convert the minimum-twist $2\to 2$ QCD jet yields (e.g., $q\bar{q}\to q\bar{q}$) into pion yields ($q\bar{q}\to\pi X$).

B. Analytic results

We begin with formal expressions for the inclusive cross sections $E\,d\sigma/d^3p$ for the process $A+B\to\pi+X$. We imagine that constituents a and b of particles A and B scatter to produce a state c plus anything. State c is either the π (as in $q\bar{q}\to\pi q$) or must fragment to produce a pion (as in $q\bar{q}\to q\bar{q}$, $q\to\pi$). In the c.m. frame of A and B, we define

$$x_R\equiv 1-\epsilon=2|\vec{p}_\pi|/\sqrt{s}\,, \tag{3.1}$$

and

$$x_t=-t/s\,, \tag{3.2}$$

$$x_u=-u/s\,. \tag{3.3}$$

Here, $t=(p_A-p_\pi)^2$ and $u=(p_B-p_\pi)^2$.

We denote by $G_{a/A}(x_a)dx_a$ the probability of finding a constituent a (in incident hadron A) with momentum fraction between x_a and x_a+dx_a.

In the case of a minimum-twist $2\to 2$ hard-scattering process such as $q\bar{q}\to q\bar{q}$, $q\to\pi$, the inclusive yield is[35]

$$E_\pi\frac{d\sigma}{d^3p_\pi}=\int_0^1 dx_a\int_0^1 dx_b\,G_{a/A}(x_a)G_{b/B}(x_b)\,\frac{1}{\pi}\,\frac{d\sigma}{d\hat{t}}\,\frac{G_{\pi/c}(z)}{z^2}\,dz\,\theta(1-z)\Big|_{z=x_t/x_b+x_u/x_a}. \tag{3.4}$$

We now adopt simple forms for the distribution functions:

$$x_iG_{i/I}(x_i)=(1+g_i)\Lambda_{i/I}(1-x_i)^{g_i} \tag{3.5}$$

and we express the $2\to 2$ hard-scattering cross section in the form

$$\frac{1}{\pi}\,\frac{d\sigma}{d\hat{t}}=D_{2\to 2}\hat{s}^{-2}(\hat{x}_t)^{-T}(\hat{x}_u)^{-U}. \tag{3.6}$$

After inserting Eqs. (3.5) and (3.6) into Eq. (3.4), we specialize to $x_F=0$. In the limit that $x_R\to 1$, we may obtain a simple analytic result[35]:

$$E_\pi\frac{d\sigma}{d^3p}=\frac{\epsilon^{g_a+g_b+g_c+2}}{p_T^4}D_{22}\Lambda_{a/A}\Lambda_{b/B}\Lambda_{\pi/c}\times 2^{g_a+g_b+T+U-2}\,\frac{\Gamma(g_a+2)\Gamma(g_b+2)\Gamma(g_c+2)}{\Gamma(3+g_a+g_b+g_c)}. \tag{3.7}$$

Neglected terms are of higher order in ϵ.

When the fragmentation of c is not present, as in the case of our high-twist processes $q\bar{q}\to\pi G$

and $qG \to \pi q$, Eq. (3.4) is replaced by

$$\frac{E_\pi d\sigma}{d^3p_\pi} = \int_0^1 dx_a \int_0^1 d\boldsymbol{x}_b G_{a/A}(x_a) G_{b/B}(x_b) \times \frac{1}{\pi}\frac{d\sigma}{d\hat{t}}\,\delta\left(1-\frac{x_t}{x_b}-\frac{x_u}{x_a}\right). \quad (3.8)$$

Expressing the high-twist (HT) cross sections in the form

$$\frac{1}{\pi}\frac{d\sigma}{d\hat{t}} = D_{\rm HT}\,\hat{s}^{-3}(\hat{x}_t)^{-T}(\hat{x}_u)^{-U}, \quad (3.9)$$

and evaluating Eq. (3.8) at $x_F = 0$ in the limit $x_R \to 1$, we obtain

$$\frac{E\,d\sigma}{d^3p} = \frac{\epsilon^{g_a+g_b+1}}{p_T^{\,6}} D_{\rm HT}\Lambda_{a/A}\Lambda_{b/B} \times \frac{\Gamma(g_a+2)\Gamma(g_b+2)}{\Gamma(2+g_a+g_b)}\,2^{g_a+g_b+T+U-4}. \quad (3.10)$$

It is instructive to examine the *ratio* of the high-twist to minimum-twist results. We begin with the contributions of the $q\bar{q}$ processes in $\pi^- N \to \pi X$. For the high-twist reaction $\bar{q}q \to G\pi^-$, a comparison of Eqs. (2.35) and (3.9) permits the identifications

$$D_{\rm HT} = \frac{8s_0\alpha_s^{\,3}}{81\pi} = \frac{128\pi f_\pi^{\,2}}{81}\alpha_s^{\,3}, \quad (3.11)$$

and

$$T = (2, 0) \quad \text{with } U = (0, 2). \quad (3.12)$$

For the minimum-twist process $\bar{q}q \to \bar{q}q$,

$$\frac{1}{\pi}\frac{d\sigma}{d\hat{t}} = \frac{4\alpha_s^{\,2}}{9}\frac{1}{\hat{x}_t^{\,2}}(1+\hat{x}_u^{\,2}). \quad (3.13)$$

Thus,

$$D_{2\to 2} = \tfrac{4}{9}\alpha_s^{\,2} \quad (3.14)$$

and

$$T = 2, \quad \text{with } U = (0, -2).$$

Using symbol $R_{q\bar{q}}$ to denote the ratio of high-twist to minimum-twist contributions to the cross section at $x_F = 0$, we find that

$$R_{q\bar{q}}(x_F = 0) = \frac{32\pi f_\pi^{\,2}\alpha_s\,\Gamma(3+g_a+g_b+g_c)}{45p_T^{\,2}(1-x_R)^{g_c+1}\Lambda_{\pi/c}\,\Gamma(g_c+2)\Gamma(2+g_c+g_b)}. \quad (3.15)$$

An extra factor of 2 was inserted in the denominator of Eq. (3.15) to account for the fact that the pion may arise from the fragmentation of either of the final quarks in $q\bar{q} \to q\bar{q}$.

In Eq. (3.15), the ratio of Γ functions represents the numerical enhancement associated with "trigger bias," and the factor $(1-x_R)^{-1-g_c}$ indicates explicitly the manner in which high-twist effects grow in relative importance as x_R is increased. For fixed s, the higher-twist terms are most important for *large* p_T.

Typical numerical values are $g_a(\pi \to \bar{q}) = 2$, $g_b(N \to q) = 3$, and $g_c = 2$. Thus, the ratio of Γ functions is 84. Furthermore, choosing $\Lambda_{\pi/c} = 0.2$, $\alpha_s = 0.25$, and $f_\pi = 0.093$ GeV, we find that

$$R_{q\bar{q}} \simeq \frac{8.1}{s x_R^{\,2}(1-x_R)^3}. \quad (3.16)$$

At $x_R = 0.75$, the value of $R \simeq 920/s$, where s is in GeV^2 units and, at $x_R = 0.90$, $R \simeq 10^4/s$. Equation (3.16) shows that the high-twist correction to $q\bar{q} \to \pi^- X$ is expected to be very substantial for all $x_R > 0.5$. For values of $s \lesssim 100$ GeV^2, the high-twist effect may predominate even for the intermediate values of x_R at which data are frequently obtained.

A similar exercise may be carried out for the high-twist $qG \to \pi q$ modification to $qG \to qG$, with $q \to \pi$ or $G \to \pi$. While the steeply falling gluon distribution function yields an increased trigger bias relative to the $q\bar{q}$ case, this is more than offset by the reduced size of the squared matrix element for $qG \to q\pi$, as discussed in Sec. II C. The result of all factors is a reduction in the relative importance of the higher-twist contribution for qG initial states. We find

$$R_{qG} \simeq \frac{1.4}{s x_R^{\,2}(1-x_R)^3}. \quad (3.17)$$

C. Numerical results

The analytic expressions in Eqs. (3.7) and (3.10) are precise only in the limit of large x_R. Because data are available principally in the region of $x_R \lesssim 0.5$, we have also employed numerical integration procedures to evaluate Eqs. (3.4) and (3.8) for a range of values of x_R and for three choices of the lab angle of the final pion. In obtaining these numerical results, we used parton densities with somewhat more structure than the simple power-law form of Eq. (3.5). In particular, for nucleon densities, we chose the scaling quark distribution functions of Field and Feynman.[36] For densities in pions, we selected

$$x d_{\pi^-}(x) = x\bar{u}_{\pi^-}(x) = 0.6(1-x)^2. \quad (3.18)$$

We believe the power $p = 2$ in $(1-x)^p$ is a correct representation of the *scaling* behavior. The form with $p \simeq 1$ found in some phenomenological fits[37] probably represents an average of the scaling minimum-twist $(1-x)^2$ contribution and the large constant high-twist piece calculated by Berger and Brodsky.[18] We ignore sea distributions in the

pion. This is not a restrictive approximation inasmuch as sea quarks are fairly ineffective at producing scattering at large p_T. At any rate, details of the pion densities do not greatly affect *comparisons* of high-twist and minimum-twist $2 \to 2$ results. (Note the cancellation of $\Lambda_{a/A}$ and factors of g_a in Eq. (3.15)]. For the gluon densities, we use the counting-rule expectations

$$xG_N(x) = 3(1-x)^5 \tag{3.19}$$

and

$$xG_\pi(x) = 2(1-x)^3 . \tag{3.20}$$

For fragmentation functions, we adopt the cascade formalism of Field and Feyman, except that we use an elementary branching function $f(\eta)$ which vanishes for $\eta \to 0$. That is, we identify $z = 1$ hadron production with specific higher-twist mechanisms and not with universal hadronization. We select

$$D_d^{\pi^-} = D_{\bar{u}}^{\pi^-} = D_{\bar{d}}^{\pi^+} = D_u^{\pi^+} \equiv D_F(z) \quad \text{(favored)}, \tag{3.21}$$

$$D_d^{\pi^+} = D_{\bar{u}}^{\pi^+} = D_{\bar{d}}^{\pi^-} = D_u^{\pi^+} = D_{s,\bar{s}}^{\pi^\pm} \equiv D_U(z) \quad \text{(unfavored)}.$$

Following Field and Feyman, we adopt

$$D_F(z) = 0.16\bar{F}(z) + 0.40 f(1-z), \qquad D_U(z) = 0.16\bar{F}(z), \tag{3.22}$$

with

$$f(\eta) = (d+1)\eta^d \Rightarrow \bar{F}(z) = \frac{d+1}{z}(1-z)^{d+1}. \tag{3.23}$$

We use $d = 2$ in our calculations. For gluon fragmentation we take

$$D_G^\pi(z) = \tfrac{4}{5}(1-z)^3/z . \tag{3.24}$$

Because we have ignored scaling violations and primordial transverse-momentum fluctuations, the inclusive cross sections take on the simple scaling form

$$E\,d^3\sigma/dp^3 = p_T^{-4} f(x_R, \cos\theta) \quad (2 \to 2 \text{ QCD}) = p_T^{-6} h(x_R, \cos\theta) \quad \text{(higher twist)}. \tag{3.25}$$

Our numerical considerations will be restricted to $\pi^- N \to \pi^\pm X$; θ is the c.m. angle between the pions. We will use the fixed coupling $\alpha_s = 0.25$ in all calculations.

As in Sec. III B, we first investigate

$$\bar{u}_\pi d_N \to \pi^- X \tag{3.26}$$

and

$$\bar{u}_\pi G_N \to \pi^- X. \tag{3.27}$$

Specifically, in the full hard-scattering expansions in Eqs. (3.4) and (3.8), we consider only those

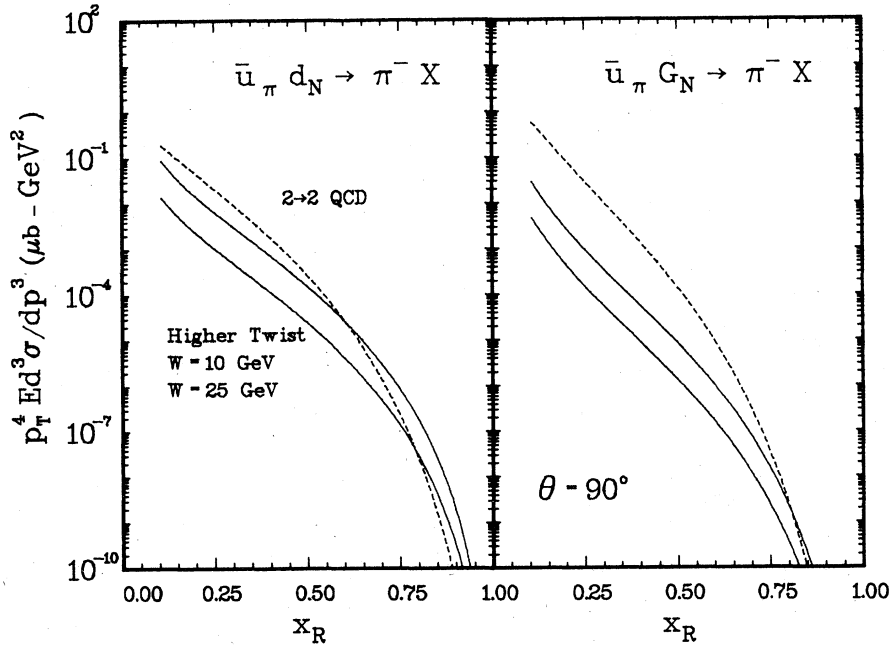

FIG. 5. Cross sections at 90° for $\bar{u}_\pi d_N \to \pi^- X$, $\bar{u}_\pi G_N \to \pi^- X$ for minimum-twist $2 \to 2$ QCD (dashed curves) and the higher-twist mechanisms of Sec. II A (solid curves). The higher-twist results scale as s^{-1}; we show results for $W \equiv \sqrt{s} = 10$ and 25 GeV.

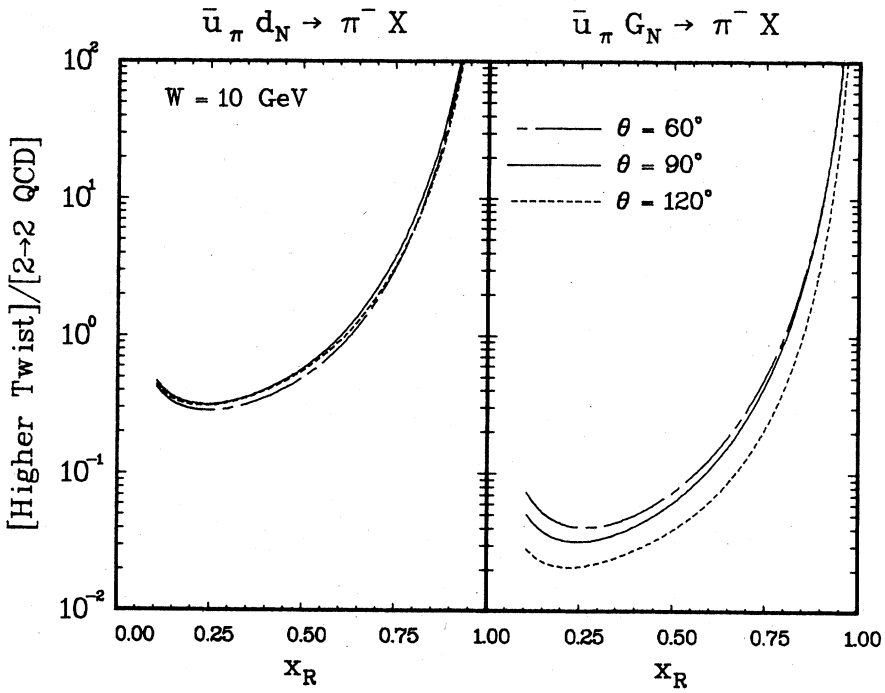

FIG. 6. Ratios of higher-twist to minimum-twist contributions for $\bar{u}_\pi d_N \to \pi^- X$ and $\bar{u}_\pi G_N \to \pi^- X$ at various scattering angles. The curves scale as $s^{-1} = W^{-2}$.

terms corresponding to $\bar{u}d$ and $\bar{u}G$ initial states. In the $2 \to 2$ minimum-twist QCD expressions, we sum over both fragmentation sequences, e.g.,

$$\bar{u}d \to \bar{u}d,\ d \to \pi^-, \qquad \bar{u}d \to \bar{u}d,\ \bar{u} \to \pi^-. \tag{3.28}$$

In Fig. 5 we show results for $p_T^4 E\, d^3\sigma/dp^3$ at $\theta = 90°$. According to Eq. (3.25), the higher-twist curves scale as s^{-1}. We provide results for $W \equiv \sqrt{s} = 10$ and 25 GeV. In Fig. 6 we show ratios of higher-twist-to-minimum-twist cross sections for $\sqrt{s} = 10$ GeV and $\theta = 60°$, 90°, and 120°. We note that the higher-twist corrections are roughly an order of magnitude more important for $q\bar{q}$ than for qG, in agreement with the discussions in Secs. II C and III B. For $W = 10$ GeV, the higher-twist term is at least a 30% correction to $\bar{u}d$ scattering for all x_R, and, in fact, it dominates for $x_R \gtrsim 0.65$.

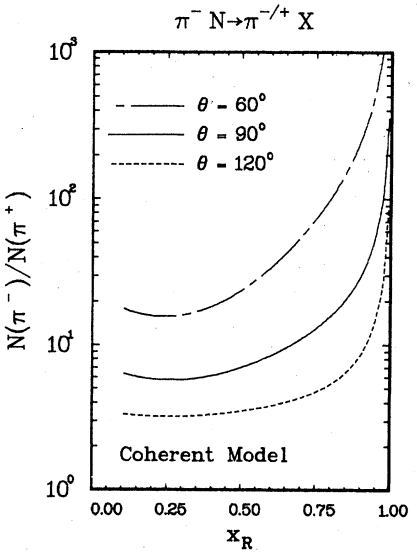

FIG. 7. Charge ratios $N(\pi^-)/N(\pi^+)$ for $\pi^- N \to \pi^\pm X$ for the higher-twist mechanisms of Sec. II A.

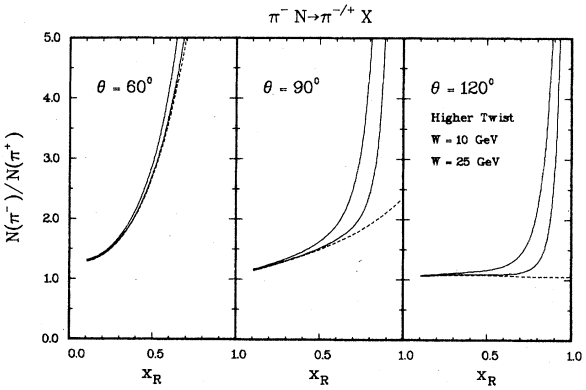

FIG. 8. Full charge-ratio predictions, Eq. (3.29), for $\pi^- N \to \pi^\pm X$. The dashed curves are the minimum-twist results, A^-/A^+.

The $\bar{u}G$, dG, and $\bar{u}d$ initial states constitute only about 20% of the total $2 \to 2$ constituent-constituent hard-scattering contributions to $\pi N \to \pi X$ and to $pN \to \pi X$. So far we have not considered GG and qq scattering and their pertinent high-twist corrections. Consequently, we cannot extrapolate directly from Figs. 5 and 6 to obtain a firm estimate of the full high-twist fraction of the signal at large p_T. The results shown in Fig. 6 are at best preliminary estimates that the high-twist fraction may well be sizable. We expect to treat qq and GG reactions in another paper.

D. Charge ratios

For the process $qG \to \pi q$, the high-twist diagrams in Fig. 2 show that the initial quark necessarily emerges from the diagrams as one of the constituents of the final pion. For $\bar{q}q \to \pi G$, both of the initial constituents emerge as constituents of the final pion. Among the higher-twist processes under consideration, the only mechanism for the charge-changing reaction $\pi^- N \to \pi^+ X$ is $G_\pi u_N \to \pi^+ \bar{d}$. According to Sec. II C, this process is relatively suppressed, particularly for small θ. Thus, we expect substantial "charge retention," viz., $N(\pi^-)/N(\pi^+) \gg 1$, for the higher-twist processes. Our explicit results are shown in Fig. 7, where we present charge ratios for the higher-twist mechanisms alone.

The large charge retention shown in Fig. 7 is also typical of constituent interchange mechanisms.[27] The failure of data to show such dramatic asymmetries is evidence against the dominance of CIM terms in high-p_T physics. We emphasize, however, that the higher-twist terms considered in this paper are not an "alternative" to conventional QCD, but rather, a correction—of fixed magnitude—required by the perturbative expansion itself. The total charge-ratio signal to be compared with data is of the form

$$\frac{N(\pi^-)}{N(\pi^+)} = \frac{A^-(x_R,\theta) + B^-(x_R,\theta)/s}{A^+(x_R,\theta) + B^+(x_R,\theta)/s} . \tag{3.29}$$

The functions $A^\mp$ represent the minimum-twist terms of $2 \to 2$ QCD, and the terms $B^\mp/s$ represent higher-twist contributions. In Fig. 8 we present our results for Eq. (3.29) for three scattering angles. The dashed curves show the minimum twist predictions, A^-/A^+. We remark that (i) for fixed s, the higher-twist effects are unimportant for small x_R, but dominant for $x_R \to 1$, and (ii) for fixed x_R, higher-twist effects decrease with increasing s, roughly as s^{-1}.

The data at $\theta = 90°$ agree with our expectations,[28] but new data at higher x_R would be telling. The $\theta = 60°$ panel in Fig. 8 deserves special comment. The large charge ratio for the minimum-twist QCD approach results from (i) strong forward poles in $qq \to qq$ elementary cross sections, and (ii) strong flavor retention in the fragmentation functions, Eqs. (3.21) and (3.22). In contrast, preliminary experimental[28] results indicate a charge ratio $N(\pi^-)/N(\pi^+) \sim 1$ for these forward scattering angles. For the reasons discussed above, our higher-twist corrections to πN *scattering* cannot rectify this disagreement.

If data continue to differ substantially from the $\theta = 60°$ expectations shown in Fig. 8, a possible explanation might be sought in the charge-retention properties of fragmentation functions. The fragmentation functions in Eqs. (3.22) and (3.23) are deduced from minimum-twist phenomenological fits to relatively low-energy data, including the deep-inelastic process $\nu N \to \mu \pi^\pm X$, for $W \sim 4$ GeV. Higher-twist contributions could well be sizable in these data.[14,19,23] It may be necessary to remove *expected*, *charge-retaining* higher-twist effects[19] from the data *before* fitting to extract the minimum-twist fragmentation functions $D(z)$.

E. Inclusive spin-spin asymmetries

In experiments with polarized proton beams and polarized targets,[38] we can define an inclusive spin-spin asymmetry

$$A_{LL} = \frac{d\sigma(p(+)p(+) \to \pi X) - d\sigma(p(+)p(-) \to \pi X)}{d\sigma(p(+)p(+) \to \pi X) + d\sigma(p(+)p(-) \to \pi X)} , \tag{3.30}$$

where the + and − refer to proton helicities. The importance of these measurements in the context of the QCD-based hard-scattering model is discussed in Refs. 29 and 30.

We would like to note briefly here that the two processes we are considering have rather simple spin structure. For $q(h_1)\bar{q}(h_2) \to \pi G$ a simple calculation shows that the color-averaged squared matrix elements are

$$F_c(--) = F_c(++) = 0, \tag{3.31}$$

$$F_c(-+) = F_c(+-) = \tfrac{1}{2} g^6 f_\pi^2 \tfrac{32}{81} \left(\frac{\hat{s}}{\hat{u}^2} + \frac{\hat{s}}{\hat{t}^2} \right) . \tag{3.32}$$

For $q(h)G(\lambda) \to \pi q$ we find

$$F_c(++) = g^6 f_\pi^2 \tfrac{4}{27} \left(-\frac{\hat{t}}{\hat{s}^2} \right), \tag{3.33}$$

$$F_c(+-) = g^6 f_\pi^2 \tfrac{4}{27} \left(-\frac{\hat{t}}{\hat{u}^2} \right). \tag{3.34}$$

At the constituent level, both processes have a fundamental asymmetry $a_{LL} < 0$. This is opposite in sign to the fundamental asymmetry of the minimum-twist process $qG \to qG$. The importance of this result depends on features of the spin-weight-

ed distribution functions for a proton. To the extent that gluon helicities are correlated with proton helicities, there will be the possibility of x_T-dependent cancellations between the negative asymmetry of $qG \to \pi q$ and the positive asymmetry of $qG \to qG$.

IV. DISCUSSION AND CONCLUSIONS

There is a growing awareness of the relevance of higher-twist phenomena in quantum chromodynamics. The inclusion of such terms affects the interpretation of Q^2 dependence in all constituent scattering processes. Some phenomena, such as longitudinal-polarization effects in deep-inelastic scattering[19,23] and in the Drell-Yan process[18] appear to require higher-twist terms with specified, relatively large normalization. Moreover, these processes are quite amenable to higher-twist analysis in that the underlying minimum-twist process is quite simple, and because simple observables exist (e.g., longitudinal polarization in the Drell-Yan process) which are sensitive to higher-twist effects in experimentally *accessible* regions of phase space.

For high-p_T production in hadron-hadron collisions the situation is more complex. To begin with, the minimum-twist QCD contribution is not based on one simple underlying elementary process. It involves a sum over many such terms. In addition, the most naive minimum-twist predictions for high-p_T processes do not agree well with experiment. Currently available data show an approximate power-law behavior

$$E\frac{d^3\sigma}{dp^3}(hN \to \pi X) \sim p_T^{-N} f(x_T)$$

with a power $N \sim 6$–8. This relatively large value of N has led many to advocate the importance of higher-twist phenomena—primarily in the context of constituent-interchange models.[13,27]

In this paper, we have evaluated the processes $q\bar{q} \to \pi G$ and $qG \to q\pi$, emphasizing the natural role of these processes in the framework of perturbative QCD. Our normalization procedure does not rest heavily on specific assumptions about the pion wave function. Viewed as corrections to the "inclusive pion yields," $\bar{q}_A q_B \to \pi X$, $qG \to \pi X$, we find that the process $q\bar{q} \to \pi G$ is quite significant, whereas $qG \to q\pi$ is less important. For both processes, the higher-twist contributions are greatest at large p_T for fixed $\sqrt{s}$. The region $x_T \to 1$ should be dominated by higher-twist phenomena of the type considered here, but it is very hard to reach this region experimentally.

We remark that our normalization procedure is identical to that used by Farrar and Fox[24] in their study of $q\pi \to q\pi$, and by Brodsky and Lepage[16] in their investigations of the pion electromagnetic form factor $F_\pi(Q^2)$. Farrar and Fox found that $q\pi \to q\pi$ is of relatively negligible importance for high-p_T processes, whereas we find that $q\bar{q} \to \pi G$ and $qG \to \pi q$ should not be ignored.

Our calculations must be combined with quantitative estimates of other high-twist effects (for example those associated with $qq \to \pi qq$) in order to obtain the full high-twist "correction" to large p_T observables. The mechanisms we consider can give rise to charge ratios in $\pi^- N \to \pi^\pm X$ which are substantially larger than unity. However, when we include the usual lowest-order, minimum-twist QCD processes, our results are consistent with data on this ratio measured at 90° in the hadron center of mass. The higher-twist contributions do not dominate the x_T region of present data ($x_T \lesssim 0.5$). Nevertheless, owing to trigger bias, the region of x_T influenced significantly by high-twist terms is larger than the region in x_F for Drell-Yan production or in z for deep-inelastic scattering. Charge-ratio data and spin-correlation measurements appear to offer the best chance to isolate high-twist effects at large p_T.

ACKNOWLEDGMENT

This work was perfomed under the auspices of the United States Department of Energy.

APPENDIX: COLOR AND COLOR PROJECTIONS

Consider the process $q_A(i, P_1)\bar{q}_B(j, P_2) \to q_A(k, P_3)\bar{q}_B \times (l, P_4) G(a, P_5)$ with the Feynman diagrams as specified in Fig. 2. It is instructive to consider separately the color factors associated with these diagrams. These are

$$\begin{aligned} C_1 &= (T^b T^a)_{ik} T^b_{lj}, \\ C_2 &= (T^a T^b)_{ik} T^b_{lj}, \\ C_3 &= T^b_{ik} (T^a T^b)_{lj}, \\ C_4 &= T^b_{ik} (T^b T^a)_{lj}, \\ C_5 &= if^{abc} T^b_{ik} T^c_{lj}, \end{aligned} \tag{A1}$$

where the T's and the f's form the fundamental and adjoint representation of SU_3, respectively. The normalization conventions are defined in Ref. 6. In addition we can specify that the final $q_A(k, P_3)\bar{q}_B(l, P_4)$ are in a color singlet by using the projection operator $P_{kl} = (1/\sqrt{3})\,\delta_{kl}$. This projection gives color factors proportional to T^a as specified below:

$$C_1^s = -\frac{1}{6\sqrt{3}}\,T_{ij}^a,$$

$$C_2^s = \frac{4}{3\sqrt{3}}\,T_{ij}^a,$$

$$C_3^s = -\frac{1}{6\sqrt{3}}\,T_{ij}^a, \qquad \text{(A2)}$$

$$C_4^s = \frac{4}{3\sqrt{3}}\,T_{ij}^a,$$

$$C_5^s = -\frac{3}{2\sqrt{3}}\,T_{ij}^a.$$

In order to calculate cross sections, we need the factors

$$C_{IJ} = \sum_{\text{colors}} C_I C_J^*. \qquad \text{(A3)}$$

With the C_I given by (A1) the C_{IJ} are

$J \backslash I$	1	2	3	4	5
1	$\frac{8}{3}$	$-\frac{1}{3}$	$-\frac{2}{3}$	$\frac{7}{3}$	3
2	$-\frac{1}{3}$	$\frac{8}{3}$	$\frac{7}{3}$	$-\frac{2}{3}$	-3
3	$-\frac{2}{3}$	$\frac{7}{3}$	$\frac{8}{3}$	$-\frac{1}{3}$	-3
4	$\frac{7}{3}$	$-\frac{2}{3}$	$-\frac{1}{3}$	$\frac{8}{3}$	3
5	3	-3	-3	3	6

(A4)

With the color-singlet projected color factors of (A2) we have for the C_{IJ}^s

$J \backslash I$	1	2	3	4	5
1	$\frac{1}{27}$	$-\frac{16}{27}$	$-\frac{16}{27}$	$\frac{1}{27}$	$\frac{1}{3}$
2	$-\frac{16}{27}$	$\frac{64}{27}$	$\frac{64}{27}$	$-\frac{16}{27}$	$-\frac{8}{3}$
3	$-\frac{16}{27}$	$\frac{64}{27}$	$\frac{64}{27}$	$-\frac{16}{27}$	$-\frac{8}{3}$
4	$\frac{1}{27}$	$-\frac{16}{27}$	$-\frac{16}{27}$	$\frac{1}{27}$	$\frac{1}{3}$
5	$\frac{1}{3}$	$-\frac{8}{3}$	$-\frac{8}{3}$	$\frac{1}{3}$	3

(A5)

If the momentum-dependent portion of the Feynman amplitudes were unimportant ($M_I = M_J$ for $I, J = 1, \ldots, 5$), then the normalization of physical cross sections would be determined *only* by the color factors (A4) and (A5):

$$\frac{d\sigma(q_A\bar{q}_B \to (q_A\bar{q}_B)G)_{\text{summed}}}{d\sigma(q_A\bar{q}_B \to (q_A\bar{q}_B)G)_{\text{singlet}}} \xrightarrow[M_I = M_J]{} \frac{\sum C_{IJ}}{\sum C_{IJ}^s} = \frac{22}{25/27}. \qquad \text{(A6)}$$

With these crude approximations, the formation of color singlets from the $q\bar{q}$ would be strongly suppressed. If (A6) were valid it would be hard to understand how color-singlet clusters of quarks, antiquarks, and gluons could ever form. If this type of suppression operated in perturbation theory, then the assumed confinement mechanism (whatever it is) would have to overcome the cancellation in order to eventually form hadrons. Final states would then be enormously sensitive to the interplay between perturbative and nonperturbative effects.

In fact, when we calculate the total matrix elements instead of just looking at color factors, things change dramatically. For a low-mass $q\bar{q}$ pair in the recombined model of Sec. II we get

$$\frac{d\sigma(q_A\bar{q}_B \to (q_Aq_B)G)_{\text{summed}}}{d\sigma(q_A\bar{q}_B \to (q_Aq_B)G)_{\text{singlet}}} = \frac{9}{4}\,\frac{(\cos^2\theta+7)(\cos^2\theta+15)}{(\cos^2\theta+9)(3\cos^2\theta+25)} = 1.05 \quad (\cos\theta = 0). \qquad \text{(A7)}$$

It is clear that instead of suppressing color-singlet $q\bar{q}$ clusters, perturbation theory favors singlets over octets here. This is consistent with the simple notion of perturbative preconfinement espoused by Veneziano and others.[33] Confinement does not have to drastically change simple perturbation estimates.

*Present address: California Institute of Technology, Pasadena, California 91125.

[1]R. D. Field, Phys. Rev. Lett. 40, 997 (1978); R. P. Feynman, R. D. Field, and G. C. Fox, Phys. Rev. D 18, 3320 (1978).

[2]S. D. Ellis and M. Kislinger, Phys. Rev. D 9, 2027 (1974).

[3]J. F. Owens, E. Reya, and M. Glück, Phys. Rev. D 18, 1501 (1978); J. F. Owens and J. D. Kimel, *ibid.* 18, 3313 (1978).

[4]A. P. Contogouris, R. Gaskell, and S. Papadopoulos, Phys. Rev. D 17, 2314 (1978).

[5]B. Combridge, J. Kripfganz, and J. Ranft, Phys. Lett. 70B, 234 (1977).

[6]R. Cutler and D. Sivers, Phys. Rev. D 16, 679 (1979); 17, 196 (1978).

[7]J. Ellis, in *Proceedings of 1979 International Symposium on Lepton and Photon Interactions at High Energies, Fermilab,* edited by H. D. I. Abarbanel and T. B. W. Kirk (Fermilab, Batavia, Illinois, 1980), p. 412.

[8]H. D. Politzer, Phys. Lett. 70B, 430 (1977); R. K. Ellis *et al.*, Nucl. Phys. B152, 285 (1979); S. Libby and G. Sterman, Phys. Rev. D 18, 3252 (1978); D. Amati, R. Petronzio, and G. Veneziano, Nucl. Phys. B140, 54 (1978).

[9]For a comprehensive review, see M. Jacob, in *EPS International Conference on High Energy Physics, Geneva, 1979* (CERN, Geneva, 1979), Vol. 2, p. 473.

[10]R. K. Ellis, M. Furman, H. Haber, and I. Hinchliffe, Nucl. Phys. B173, 397 (1980).

[11]This form is discussed, for example, by S. J. Brodsky, in *Quantum Chromodynamics,* proceedings of the Summer Institute on Particle Physics, SLAC, 1979, edited by Anne Mosher (SLAC, Stanford, 1980).

[12]H. D. Politzer, Nucl. Phys. B172, 349 (1980).

[13]R. Blankenbelcer, S. J. Brodsky, and J. F. Gunion, Phys. Rev. D 18, 900 (1978); R. Horgan, W. Caswell, and S. J. Brodsky, *ibid.* 18, 2415 (1978).
[14]E. L. Berger, Z. Phys. C 4, 289 (1980).
[15]D. J. Gross and S. B. Treiman, Phys. Rev. D 4, 1059 (1971); S. Gottlieb, Nucl. Phys. B139, 125 (1978).
[16]G. P. Lepage and S. J. Brodsky, Phys. Rev. D 22, 2157 (1980) and many references therein.
[17]M. Jacob and P. Landshoff, Phys. Rep. 48, 285 (1978).
[18]E. L. Berger and S. J. Brodsky, Phys. Rev. Lett. 42, 940 (1979).
[19]E. L. Berger, Phys. Lett. 89B, 241 (1980).
[20]G. Farrar and D. Jackson, Phys. Rev. Lett. 35, 1416 (1975); A. I. Vainshtein and V. I. Zakharov, *ibid.* 72B, 368 (1978).
[21]G. Farrar and D. Jackson, Phys. Rev. Lett. 43, 246 (1979); see also Z. F. Ezawa, Nuovo Cimento 23A, 271 (1974).
[22]K. J. Anderson *et al.*, Phys. Rev. Lett. 43, 1219 (1979).
[23]CERN-Milano-Orsay Collaboration, C. Matteuzzi, report presented at XX International Conference on High Energy Physics, Madison, Wisconsin, 1980 (unpublished) and CERN Report No. CERN/EP/80-124 (unpublished).
[24]G. Farrar and G. C. Fix, Nucl. Phys. B167, 205 (1980).
[25]J. Gunion, University of California, Davis report, presented at the Discussion Meeting on Large Transverse Momentum Phenomena, SLAC, 1978 (unpublished).
[26]K. P. Das and R. Hwa, Phys. Lett. 68B, 459 (1977).
[27]J. Gunion and D. Jones, Phys. Rev. D 20, 232 (1979).
[28]Chicago-Princeton E-258 Collaboration, H. J. Frisch, in *Quantum Chromodynamics*, proceedings of the Summer Institute on Particle Physics, SLAC, 1979, edited by Anne Mosher (SLAC, Stanford, 1980).
[29]J. Babcock, E. Monsay, and D. Sivers, Phys. Rev. Lett. 40, 1161 (1978); Phys. Rev. D 19, 1483 (1979); K. Hidaka, E. Monsay, and D. Sivers, *ibid.* 19, 1503 (1979).
[30]J. Ranft and G. Ranft, Phys. Lett. 77B, 309 (1978); H. Cheng and E. Fishback; Phys. Rev. D 19, 860 (1979); K. Hidaka, *ibid.* 21, 1316 (1980).
[31]T. DeGrand and H. Miettinen, Phys. Rev. Lett. 40, 612 (1978).
[32]D. W. Duke and F. E. Taylor, Phys. Rev. D 17, 1788 (1978); Van Chang and R. C. Hwa, Phys. Lett. 85B, 285 (1979); L. M. Jones, K. E. Lassila, U. Sukhatme, and D. Willen, Phys. Rev. D (to be published).
[33]D. Amati and G. Veneziano, Phys. Lett. 83B, 87 (1979).
[34]T. Gottschalk and D. Sivers, Phys. Rev. D 21, 102 (1980).
[35]S. J. Brodsky, T. DeGrand, J. Gunion, and J. Weis, Phys. Rev. D 19, 1418 (1979).
[36]R. Field and R. Feynman, Phys. Rev. D 15, 2590 (1979).
[37]C. B. Newman *et al.*, Phys. Rev. Lett. 42, 951 (1979).
[38]I. P. Auer *et al.*, Argonne Report No. ANL-HEP-CP-80-38 (unpublished).